Proceedings of the Second International Workshop on EGS, 8.-12. August 2000, Tsukuba, Japan
KEK Proceedings 200-20, pp.74-91

Dosimetric Characterization of Low Energy Brachytherapy Sources: An EGS4 Monte Carlo Study

E. Mainegra and R. Capote

Departamento de Física,
Centro de Estudios Aplicados al Desarrollo Nuclear,
Calle 30 #502, e/ 5ta y 7ma, Miramar, La Habana, Cuba

Abstract

An exhaustive revision of dosimetry data for low energy interstitial brachytherapy sources has been performed by means of the EGS4 Simulation System. DLC-136/PHOTX cross section library, water molecular form factors, bound Compton scattering and Doppler broadening of the Compton-scattered photon energy were considered in the calculations. Two-dimensional dose rate distributions in water and air-kerma strength around ^{103}Pd model 200 and ^{125}I models 6702 and 6711 were calculated, allowing dose rate constants (DRC) Λ, radial dose functions $g(r)$ and anisotropy functions $F(r,\theta)$ to be estimated. Influence of calibration procedure on source strength for low-energy brachytherapy seeds is discussed. A theoretical estimate of the DRC for ^{103}Pd model 200 seed equal to 0.669$\pm$0.002 cGyh^{-1}U^{-1} was obtained. Radial dose functions $g(r)$ were extensively compared with experimental as well as with theoretical results. Binding corrections for Compton scattering have a negligible effect on radial dose function for ^{103}Pd seeds under 5.0 cm from source center and for ^{125}I seed model 6702 under 8.0 cm. Solid water results underestimate radial dose function for low-energy sources by as much as 6 % for ^{103}Pd and 2.5 % for ^{125}I already at 2 cm from source center. Anisotropy functions $F(r,\theta)$ were compared against a limited set of measured data selected from the literature and other Monte Carlo results. Binding corrections and phantom material selection have been found to have no influence on the anisotropy function. A right cylindrical model of the titanium container seems to overestimate the anisotropy for angles below 20-30 degrees.

1 Introduction

Accurate knowledge of two-dimensional dose distribution around radioactive sources employed in interstitial brachytherapy implants is necessary in order to provide a solider basis when developing a clinical strategy. In the past fifteen years experimental and theoretical studies on the dosimetry of brachytherapy sources have been undertaken intensively. Nath *et al* [1] reviewed studies for ^{125}I seed models 6711 and 6702, and ^{103}Pd seed model 200. A great amount of data both, experimental [2-12] , and theoretical [13-25] are available to be used directly in clinical treatment planning. However, some practical as well as theoretical problems remain still open.

The numerical value of the dose rate constant depends strongly on the standardization measurements to which the air-kerma strength calibration of the source is traceable. The recent history of ^{125}I sources illustrates that not even existence of NIST air-kerma strength standard is a guarantee of accuracy of Monte Carlo calculated absolute dose rates. Only by careful simulation of the original NIST free-air chamber measurements, so as to model the effect of low-energy contaminant x-rays on the standard, can experimental and Monte Carlo dosimetry be reconciled [19, 20]. Measurement of the dose distribution is usually performed in "water equivalent" solid plastic phantoms. Williamson

[20] showed that solid water does not reproduce the scattering and absorption cross sections of liquid water in the low energy range (^{125}I and ^{103}Pd sources), thus resulting in an underestimation of the radiation penetrability in water. Interstitial brachytherapy treatment planning systems often use the one-dimensional point source approximation for dose rate distribution calculations. This is a fair assumption in implants with large number of sources randomly distributed. However, anisotropy effects cannot be neglected when small number of sources regularly arranged is used, i.e., in temporary brain implants and ophthalmic plaque applications. Single seeds, especially those with average emission energy below 80 keV, present a marked anisotropy in dose distribution around the longitudinal source axis.

In this study we review the state of the art dosimetry of iodine and palladium brachytherapy seeds. Comparison with experimental and theoretical results reported in the literature will be presented to validate our calculations. Influence of calibration procedure on source strength for low-energy brachytherapy seeds is discussed. The influence of phantom material and Compton binding corrections on the radial dose and anisotropy function is studied. Limitations and advantages of Monte Carlo simulation of photon transport in predicting 2-D anisotropy functions is discussed.

2 Materials and Methods

2.1 Dose calculation formalism

We follow the dose calculation formalism proposed originally by the Interstitial Brachytherapy Collaborative Working Group [10] to predict two-dimensional dose distributions around cylindrically symmetric sources and expanded to all brachytherapy sources by the AAPM Radiation Therapy Committee Task Group No.43 [1]. The dose rate at a point (r, θ) relative to the geometric source center is given by

$$\dot{D}(r,\theta) = S_k \Lambda G(r,\theta) / G(r_0,\theta_0)\, g(r)\, F(r,\theta) \tag{1}$$

In this formalism, the air-kerma strength S_k, a measure of source strength, is specified in terms of air kerma rate at a point along the transverse axis of the source in free space. It is defined as the product of air kerma rate at a calibration distance, d, in free space $K_r(d)$, measured along the transverse bisector of the source, and the square of the distance, d. The dose rate constant, Λ, is the dose rate per unit source strength at a reference point taken here to be 1 cm from the source center on its transverse bisector. The geometry distribution $G(r,\theta)$ accounts for the variation of relative dose due to the spatial distribution of radioactivity in the source. Because the three-dimensional distribution of radioactivity within the source core is uncertain for many sources, and because the choice of geometrical factor $G(r,\theta)$ influences mainly the accuracy of interpolation, we have adopted the line source model (see Ref.[1]). The radial dose function g(r) accounts for radial dependence of photon absorption and scatter in the medium along the transverse axis ($\theta = \pi/2$). The anisotropy function $F(r,\theta)$ accounts for the angular dependence of photon absorption and scatter in the encapsulation and the medium. For a definition or more detailed description of the formalism and the quantities used, the reader is referred to the Task Group 43 report [1] or the paper by Williamson and Nath [26].

2.2 Brachytherapy sources and phantoms

For the sources studied the basic sizes and materials of the core and capsules (cladding) used in the calculations were taken as follows: ^{125}I seeds as described by Williamson [20] and ^{103}Pd seed model 200 as described by Chiu-Tsao and Anderson [12]. Energy spectra of source photons were taken from the NUDAT database [27]. In this study a cylindrical phantom was used. A brachytherapy source was located in the center of the phantom with its long axis coincident with the phantom central axis. Phantom materials included air, water and solid water. The composition by weight of solid water is stated to be hydrogen 8.0%, carbon 67.22%, nitrogen 2.4%, oxygen 19.84%, calcium 2.32%, and

chlorine 0.13% [28]. Its density was taken as 1.015 g/cm^3. An additional calculation with liquid water thin ring detector embedded in solid water phantom was done to obtain solid water-to-water correction factor. The dose calculation grid was so dimensioned that on the transverse and longitudinal axes a width of 0.02 cm under 0.1 cm, between 0.1 cm and 2.0 cm a width of 0.1 cm and beyond 2 cm a width of 0.5 cm were used.

2.3 Monte Carlo calculations

Monte Carlo calculations were performed using the EGS4 code system [29,30]. The most recent photon cross section compilation, DLC-136/PHOTX cross section library [31] contributed by the National Institute of Standards and Technology (NIST) and implemented for EGS4 use by Sakamoto [32] was employed in the calculations. This library uses the theoretical photo-effect cross section of Scoffield [33], but without renormalization for low atomic number elements. This difference between DLC-136 and its predecessors (DLC-7F, DLC-99) is very important for low-energy sources, since mean emission energy of these sources falls in the photoeffect dominated region. Bound Compton scattering and Doppler broadening of the Compton-scattered photon energy were considered in the calculations by including the Low-Energy Photon-Scattering (LSCAT) expansion for the EGS4 Code [34]. Molecular form factors from Morin [35] for coherent scattering in water as implemented by Leliveld [36] were also included. Cylindrically symmetric brachytherapy sources were modeled with a modified version of the EGS4 user code DOSRZ [37] that allows simulation of particle transport through a mesh composed by cylindrical shells and scores deposited energy in any desired shell. In addition, our Monte Carlo EGS4 user code was used to calculate the air kerma strength per unit activity for each seed model allowing clinically relevant absolute absorbed dose rates in water to be estimated.

An analog dose estimator was employed, since we adopted the original scheme of scoring deposited energy in each shell and averaging it over the mass of the cylindrical shell. Electrons were not transported and the cutoff energy for photon transport in all calculations was 1 keV (PCUT=0.001MeV). A variance reduction technique was used in which photons were not allowed to undergo photoelectric absorption, but were forced to scatter at each interaction site. The resulting bias in the dose estimator was removed by reducing the weight of the scattered photon by the branching ratio $(\sigma_{Compton} + \sigma_{pair})/(\sigma_{Compton} + \sigma_{pair} + \sigma_{photo})$ (coherent scattering in EGS4 system is treated in an independent way as a correction) and scoring a deposited energy equal to the photon energy times the initial photon weight reduced by the ratio $\sigma_{photo}/(\sigma_{Compton} + \sigma_{pair} + \sigma_{photo})$. For air kerma calculations in vacuum, particles heading to detector were split into 100 daughter particles with weight 1/100; in any other case, particles emerging from the source were discarded. The ring detector region for vacuum simulations was located 100 cm away from the source in the transverse axis direction. Inner and outer radiuses of the ring were 99.5 and 100.5 cm respectively and height of the ring was equal to 1 cm. The outer diameter of the simulation geometry is 40 cm for liquid / solid water. Air kerma strength S_k for ^{125}I model 6711 and 6702 seeds was calculated by simulating the free-air chamber calibration measurements performed at NIST [38]. The air-kerma strength S_k for ^{103}Pd was evaluated in a vacuum simulation (excluding all source spectrum radiation below 10 keV and Ti x-ray fluorescence emission). All quoted calculation errors are only statistical within 1 standard deviation.

3 Results and discussion

3.1 Dose rate constant

3.1.1 ^{125}I seeds

Table 1 compares our theoretically calculated DRC [24] with previously published results. Statistical uncertainty in all regions of interest for DRC calculations was below 0.5% for water and solid water medium and below 1% for air medium. DRC values obtained by us using the original photon cross

section compilation (DLC-15) supplied with EGS4 and those by Williamson [19] using photon cross section compilation (DLC-7F), are also reported. They show excellent agreement and reinforce the need to use up-to-date photon cross section libraries, since they can affect DRC values. As mentioned before, air-kerma strength was calculated by simulating free-air chamber calibration measurements performed at NIST by Loftus [38]. From those computed values of S_k, correction factors for attenuation in air of 0.001490 cm^{-1} and 0.001486 cm^{-1} were obtained for the seed models 6702 and 6711 respectively in excellent agreement with the 0.0015 cm^{-1} value measured by Loftus [38] and the value of 0.0014 cm^{-1} calculated by Williamson [20]. Applying air attenuation correction factors and averaging over all distances we obtained DRC values showed in table 1. Calculated DRC values for solid water medium agree with the average of the ICWG measurements [10] within 1.5% and 1.4% and with Williamson [20] calculations within 1.2% and 0.01% for the model 6711 and 6702 seeds respectively. In addition, our calculations are in agreement within 1.0% with Luxton [22] corrected DRC value obtained from lucite-medium measurement for the 6711 seed .

Using air-kerma strength calculated in vacuum we obtained a DRC value of 0.83 $cGyh^{-1}U^{-1}$ for the ^{125}I model 6702 seed. This value is in excellent agreement within 0.4% with the one obtained by Mason et al [39] and should be considered a theoretical constant based on a fundamental geometry with vacuum between the source and detector, and fully consistent with the AAPM definition [26]. This result suggests that NIST correction for air attenuation does not properly yield the air-kerma rate in free space. It is worth noticing that Ti K-edge characteristic x-rays were included in our vacuum calculations as well as in Mason et al work [39].

On January 1, 1999 NIST implemented its revised air-kerma strength standard for low-energy interstitial brachytherapy seeds. This calibrations are based upon measurements using Loevingers wide-angle free-air chamber (WAFAC) with a thin absorber to eliminate the Ti x rays [40]. The revised DRC value for model 6702 is equal 1.040 $cGyh^{-1}U^{-1}$. In a previous work we reported air-kerma strength calculations for this model in vacuum, neglecting characteristic x-ray production [24]. The obtained DRC value of 1.009 $cGyh^{-1}U^{-1}$ is 3% lower than the one of the 1999 NIST standard .

3.1.2 ^{103}Pd seed model 200

Chiu-Tsao and Anderson [12] published absolute dose rate distributions measured in solid water phantom for this seed. Their data are presented as the product of distance squared and dose rate per unit source strength in units of cm^2 cGy $h^{-1}mCi^{-1}$. This product has the value 0.680 cm^2 cGy $h^{-1}U^{-1}$ at a distance of 1 cm on the transverse axis. By definition this value is the measured DRC for ^{103}Pd seed model 200 in solid water. Meigooni et al [11] reported a value of DRC for ^{103}Pd equal to 0.735±0.03 cGy $h^{-1}U^{-1}$. The AAPM in TG-43 report recommended to average these measurements and applied a multiplicative correction factor (1.048) to convert from solid water measurement medium to a liquid water reference phantom obtaining a DRC value of 0.74 cGy $h^{-1}U^{-1}$ for the model 200 seed. Both TLD measurements were normalized by an air-kerma strength derived from the vendor's contained activity specification and deviate by 7.5%. The most likely explanation of this difference is poor reproducibility and systematic error of the vendor's activity measurement procedures. Another possible explanation for this discrepancy might be that Chiu-Tsao and Anderson [12] used homemade solid water, which may have had a slightly different composition than the commercial material used in the work of Meigooni et al [11].

We computed absorbed dose in a liquid water detector embedded in a solid water phantom and calculated S_k in vacuum, considering photon emission above 10 keV and without Ti x-ray fluorescence emission. A DRC value in solid water of 0.639±0.002 cGy $h^{-1}U^{-1}$ was obtained, being 6% smaller than Chiu-Tsao's experimental value. Our above mentioned solid water result assumes a detector calibrated for dose to water. A calculation in a solid water phantom which does not consider such calibration yielded a DRC value of 0.677±0.002 cGy $h^{-1}U^{-1}$, agreeing with Chiu-Tsao and Anderson [12] experimental value within 0.4%. Calculations in liquid water medium produced a DRC value of 0.669±0.002 cGy $h^{-1}U^{-1}$[24].

An air kerma standard for ^{103}Pd model 200 seed was introduced by NIST only in January 1999

and in 2000 new AAPM recommendations on ^{103}Pd dosimetry were published [41]. In this report the authors recommend to average a measured DRC value using TLD dosimeters in solid water by Nath *et al.* [42] of 0.650±0.050 cGy $h^{-1}U^{-1}$ with the Monte Carlo calculated DRC value performed by Williamson [43] of 0.680±0.020 cGy $h^{-1}U^{-1}$. Averaging these two estimates a DRC value of 0.665±0.030 cGy $h^{-1}U^{-1}$was recommended in the AAPM 69 report. This average value is in excellent agreement with our Monte Carlo predicted value of 0.669±0.002 cGy $h^{-1}U^{-1}$ in a previous work [24].

However, in our opinion, it is inconsistent to average DRC values obtained in different media. To account for differences between solid and liquid water results, conversion factors have been reported in the literature [20], [22], [24]. A more realistic choice can be obtained applying a correction factor to the most recent measurements by Nath *et al.* [41] as done in TG43. In this way a DRC value of 0.681±0.050 cGy $h^{-1}U^{-1}$is obtained in excellent agreement with the latest Monte Carlo calculation by Williamson [43]. This value can be considered the best selection for the DRC of ^{103}Pd seed model 200.

3.2 Radial dose functions

3.2.1 ^{125}I seeds

Radial dose functions $g(r)$ for ^{125}I seed models 6702 and 6711 have been calculated in liquid and solid water phantoms [25]. Statistical errors are smaller than 1% within one standard deviation for distances under 10 cm. From figure 1 can be seen that results are divided in two well defined trends. Values of $g(r)$ in solid water are consistently smaller than those in liquid water giving rise to differences of 4.19 % for model 6702 and 5.62 % for model 6711 already at 2.5 cm and 12.26 % for model 6702 and 14.31 % for model 6711 at 5 cm from source center. We compared our liquid water calculations with the Monte Carlo data of Burns and Raeside [17] and those of Williamson [20] finding excellent agreement. Solid water results are in good agreement with experimental measurements of Nath [7] with discrepancies smaller than 5 % (mean relative difference is 2.73 %) for model 6702 and 3.5 % (mean relative difference is 1.80 %) for model 6711 under 7 cm. We also included in the comparison the fifth order polynomial fit proposed by the ICWG [10], finding an excellent agreement under 6 cm (1.11 % mean relative error) for model 6702. The difference is progressively larger over this distance and a somewhat worse agreement is obtained for model 6711 with 6 % relative difference at 5cm (4.5 % mean relative error under 5 cm). For tabulated values of radial dose functions the reader can consult [25].

3.2.2 ^{103}Pd seed model 200

^{103}Pd sources are less studied than ^{125}I sources. Meigooni *et al* [11] and, Chiu-Tsao and Anderson [12] performed dose measurements using LiF TLD in a solid water phantom. Both results were in good agreement (within 5 %) for distances greater than 2 cm. Calculated radial dose functions [25] in liquid and solid water were compared with values obtained from the experimental results reported in [12] and the compromise chosen by the AAPM Task Group No.43 [1] of averaging the above mentioned data sets. We can see in Figure 1 (lower panel) that our results in liquid and solid water show discrepancies of 6% already at 2 cm from source center and of 10% at 3 cm. Interesting is the fact that Chiu-Tsao's results match much better our liquid water results than those in solid water. There is an excellent agreement between our results in solid water with the averaged results of these two data sets. As reported in the Task Group 43 report [1], a homemade solid water phantom was used in [12], which may have had a slightly different composition than the commercial material used in [11]. For the tabulated values of radial dose function for ^{103}Pd model 200 seed the reader can consult [25].

3.2.3 Effect of Compton binding corrections on radial dose functions

The influence of Compton binding corrections on radial dose function for all sources was investigated. As reported by Williamson [14], binding effects become non-negligible for a seed with average

emission energy below 100 keV. We will refer to the bound case when considering binding corrections and to the free case when we do not consider them. Comparing the bound case with the free approach for ^{103}Pd sources (Figure 2, upper panel) we see that up to 2.5 cm differences are under 1% between both cases, reaching 2% at 5 cm. Beyond 5 cm an increasingly larger bound to free ratio is observed. A similar behavior is observed for ^{125}I seed model 6702 (Figure 2, lower panel). Under 4.5 cm the bound to free ratio is almost 1 with differences under 1% beginning a slowly increase beyond 4.5 cm. Beyond 8 cm differences become larger than 2%. Wang and Slovoda [23] explored the influence of binding effects of Compton scattering on deposited dose along the transverse axis for ^{125}I seed model 6711. They reported bound and free results to be nearly identical (less than or equal to 1%) under 7 cm from source center and an increasingly larger bound to free ratio beyond this distance. Since we calculate the ratio between radial dose functions (see definition) our results will differ by a factor given by the ratio between dose rate at 1cm in the free case to that of the bound case. From our MC calculations we computed this factor to be 1.0102. Dividing by this factor our results of the bound to free ratio is lowered by about 1% achieving excellent agreement with [23].

3.3 Anisotropy functions

Monte Carlo calculations were performed in liquid and solid water phantoms to obtain anisotropy function for all three low-energy brachytherapy sources [44]. No influence of phantom material selection nor of the binding corrections on the anisotropy function was observed.

3.3.1 ^{103}Pd model 200 seed

Liquid and solid water medium : With its lower average photon energy, ^{103}Pd seed exhibits stronger anisotropy effects and a faster dose falloff with distance than ^{125}I sources. Therefore, it is of interest to determine the anisotropy function at very close distances from the source. Anisotropy function values calculated from the Monte Carlo simulations in liquid and solid water phantoms are shown in figure 3 as a function of distance. As can be observed from the similar results in both media, there is practically no influence of phantom material on the anisotropy function for ^{103}Pd photon energies. Although not graphically shown, calculations with and without binding corrections have been also performed finding not significant influence on the anisotropy function. An analysis at 50^o and 80^o, where statistical uncertainties are under 0.5%, showed mean relative differences between results with and without binding corrections of 0.18% and 0.11% respectively.

A strong anisotropy and a marked dependence with distance on the longitudinal axis can be observed. This dependence with distance decreases considerably already at 10^o. It can be observed that the anisotropy function along the longitudinal axis for r = 0.3 cm is equal 1.0793, i.e., 7.93 % higher than on the transverse axis at the same distance, what may be attributed to the greater proximity to one of the two active pellets in the seed [12]. Anisotropy function uncertainties due to statistical fluctuations in computed dose distributions are under 1% elsewhere excluding the longitudinal axis. Along this axis uncertainties are somewhat higher, being under 1% below 1cm, under 3% up to 3cm and around 5% over this distance.

Significant differences of our results with the experimental values [12,45] are observed below 2.5 cm from the seed. However, we are able to reproduce the physical fact that the dose on the longitudinal axis near the source is higher than that on the transverse axis, as was measured by Chiu- Tsao and Anderson [12]. The drastic increase of the anisotropy function near the source on the longitudinal axis is not observed in the experimental data reported by Nath [45], which are limited to 1 cm from the source.

Recently, Weaver [6] reported anisotropy functions for ^{103}Pd-source model 200 and for ^{125}I-source models 6702 and 6711. Data were generated through a two-step process, determining first the source intrinsic radiation emission pattern from in-air measurements at 100 cm from source center and then using these data as input to Monte Carlo calculations of the fluence distribution in water. This approach was developed in an effort to design a fast, efficient source model that would produce

accurate results, without having to propagate photons through detailed source geometry [46]. Data from this work were also included in figure 3 for comparison. The largest discrepancy with our values is found along the longitudinal source axis where Weaver's values are lower than ours and do not reproduce the physical fact that the dose on the longitudinal axis near the source is higher than that on the transverse axis. At 10^o agreement is excellent between both data sets except near the source. At higher angles Weaver's values become systematically slightly higher than ours.

Air medium : In order to understand the discrepancies observed with the results of Weaver [6] we modeled his experimental setup and simulated the procedure used to measure the angular emission distribution in air. The idea was to compare directly with measured experimental data, avoiding effects, which could be introduced by the Weaver Monte Carlo simulation. We found it necessary to model the ^{103}Pd electroplated on graphite cylinders as a 0.3 mm layer. The layer thickness was deduced by fitting Weaver's experimental results. Calculations performed in air and in vacuum produced the same result showing that contributions to the fluence by scattered radiation in air is negligible. Figure 4 shows a comparison of our Monte Carlo simulation with values from the best representation curve of the experimental fluence. Although the minimum in both data sets is located almost at the same position, our values are somewhat lower than Weaver's data. Experimental maximum is observed at 80^o and in our calculation at 87^o. Our right cylindrical model could produce the underestimation of experimental data between 20 and 40 degrees. Irregularities in source design reported by Weaver [6] and the lack of an accurate source description are likely to be the reasons for remaining discrepancies and set the limits for the prediction capability of Monte Carlo generated data for Pd-103 seed model 200.

3.3.2 ^{125}I model 6702 seed.

In this model the radioactive material is adsorbed onto three resin spheres, which can move freely inside the titanium capsule. This movement is responsible for variability in measured values even of the same source before and after movement of the source [6], making reproducibility of any measurement hard to achieve. We simulated the three active resin spheres as small fixed cylinders and assumed them to be spaced, center-to-center, at intervals of 1.1 mm. However, photon emission was modeled from a spherical surface located inside each resin cylinder. Statistical uncertainties are under 1% for any angle excluding the longitudinal axis where uncertainties are under 2.5 % for distances up to 5 cm getting up to 5 % beyond this distance.

In figure 5 we plotted anisotropy values as function of distance obtained in liquid water at four angles for distances between 0.5 cm and 9.0 cm. As for ^{103}Pd sources, there is no influence of phantom material nor of the binding corrections on the anisotropy function. We compared our results with values measured by Nath [45] in a solid water phantom and recommended as reference data by the AAPM Radiation Therapy Committee Task Group 43 [1], those of Weaver [6] combining experimental measurements of angular emission distribution with Monte Carlo simulation as mentioned before and with Monte Carlo calculated values by Williamson (private communication, 1997) using MCPT code, who simulated a 6702 seed with elliptical end welds (0.5 mm thick) and three resin balls spaced center-to-center at intervals of 1.1 mm.

Nath values appear scattered around the other data sets making it difficult to assess whether our right cylinder model or the elliptical end welds model used by Williamson are a closer representation of the real geometrical structure of the seed. Our results are about 12 % more anisotropic than those of Williamson for angles close to the longitudinal axis. These differences progressively diminish with increasing angle. This behavior is in correspondence with the geometrical models assumed since a right cylinder would affect the emitted radiation in a stronger way than a source with elliptical end welds in the region near the longitudinal axis. Values reported by Weaver are more anisotropic than ours at 0^o within 7 %, but at larger angles differences tend to vanish.

3.3.3 ^{125}I model 6711 seed.

Liquid and solid water medium : Several structural details of this model, including geometrical configuration of the capsule end welds and the shape of the axial surfaces of the silver rod, are not known precisely and the 2D dose distribution is sensitive to these factors [47]. We have used two geometrical source models with the common feature that the radioactive silver core is a right cylinder centered inside the titanium encapsulation, but photons can be emitted from the cylindrical surface disregarding source ends (partial emission) or from its whole surface (total emission). In figure 6 anisotropy function values as function of angle at three different distances are compared with values measured by Nath [45] in a solid water phantom using TLD dosimeters, with the data obtained by Weaver [6] as described earlier and with Monte Carlo calculated values fitted to a truncated Fourier series by Williamson and Quintero [47]. The latter workers assumed the silver rod to be ellipsoidal in shape and coated with a 4 mm thick layer of AgH with ^{125}I uniformly distributed over an ellipsoidal surface embedded 1 mm below its surface. We have also included the matrix fit to diode and TLD measured data of Ling [2] and the Monte Carlo calculation of Chiu-Tsao with the code MORSE [8]. The later authors modeled the silver wire as a right circular cylinder emitting photons from a uniform layer 1 mm thick, with a 1 mm standoff, over the entire surface including the cylindrical portion and the two end points.

In the results obtained using a partial emitting source no values over unity are observed. A good agreement with Williamson calculations [47] is found very close to the source excluding the region on the longitudinal axis, where our right cylinder model predicts more anisotropic values than the geometrical model used by this author of an elongated ellipsoid. Weaver data [6] show a less anisotropic dose distribution close to the source at angles near the longitudinal axis and they do not present values greater than unity. The data of Ling is limited up to 30^o and lie within the limits defined by the theoretical results[43]. In general, differences between all data sets tend to disappear at large distances. This result strongly favors the full emitting source model, therefore we selected it to produce the final results. EGS4 calculated values of the anisotropy function for the total emitting source model are presented in table 2 from 0^o to 80^o in 10^o steps and for distances between 0.5 cm and 9 cm. Statistical uncertainties are under 1% for any angle excluding the longitudinal axis where uncertainties are under 3% for distances up to 5 cm reaching 5 % below 9 cm.

Air medium : Experimental measurements of the angular emission distribution performed by Weaver [6] were simulated and the resulting in-air relative fluence is compared with the curve best representing the experimental values in figure 7. There is an excellent agreement between the experimental and the Monte Carlo calculated data. Only near the longitudinal axis between 5^o and 10^o is our data slightly lower than the experimental values. This is probable a consequence of the assumed geometrical model in our Monte Carlo calculations, although variations in source encapsulation are also possible. Weaver reported less variability in measurements performed for this seed model than for the other low energy seeds suggesting less movement in the active material. Considering the excellent agreement for the in-air relative fluence at 100 cm shown in Figure 7, we can conclude that differences observed in our calculated anisotropy function values in water with Weaver calculations near the source are mainly due to the use of an angular emission distribution measured at 100 cm. This angular distribution misses significant geometrical information about the source. This could be considered a limitation of the Weaver approach.

4 Conclusions

An exhaustive and consistent evaluation of dosimetric characteristic of commercially available ^{125}I seed models 6711 and 6702 and ^{103}Pd seed model 200 has been performed [24,25,44]. The accuracy of a Monte Carlo EGS4 simulation in the energy range from 20 to 40 keV was validated by comparing its predictions with a large set of experimental data and theoretical calculations of well characterized

^{125}I seeds. The agreement of our Monte Carlo calculations with experimental measurements, as well as with other Monte Carlo simulations, within 1.5% for DRC of ^{125}I seeds, enhances confidence in the reliability of Monte Carlo simulation as a dose-computation tool, allowing us to study other, less measured, brachytherapy sources. When a new NIST standard for ^{125}I seeds, correcting the influence of low-energy contaminant radiation is released, excellent agreement between experimental results in air, corrected for attenuation in air, and in vacuum calculations should be expected.

A DRC value for ^{103}Pd seed model 200 in liquid water medium of 0.669±0.002 cGy h^{-1}U^{-1} was obtained in 1998 [24] in excellent agreement with 0.665±0.02 cGy h^{-1}U^{-1} value recently recommended in AAPM Report 69 [41].

Monte Carlo calculated radial dose functions for ^{125}I seeds in liquid and solid water phantoms were validated against experiment and other calculations finding excellent agreement. The fifth order polynomial fit obtained by the ICWG [10] and recommended by the AAPM Task Group No.43 [1] reproduces very good our solid water calculations for both ^{125}I seed models under 5 cm.

We have studied the influence of binding corrections on the radial dose function for low-energy brachytherapy seeds. Neglecting binding effects does introduce a maximal error in radial dose function of about 2% under 5 cm for ^{103}Pd and under 8 cm for ^{125}I seeds.

Anisotropy functions near low energy sources reflect their geometrical internal details. At large distances those geometrical details become less visible. Only through detailed knowledge of seed structure can Monte Carlo calculations accurately reproduce measured relative in-air fluence. On the other side, measurements performed on several seeds for the same model can produce different outputs, introducing certain ambiguity in the experimental determination of angular dose distributions. Averaged values should be taken for clinical practice. No appreciable influence of binding effects and phantom material selection (liquid water or water-equivalent material) on the anisotropy function has been found.

Anisotropy function values for the ^{103}Pd seed model 200 obtained from our calculations and experimental values reported by Chiu-Tsao reproduce the physical fact of an increase in the anisotropy function on the longitudinal axis towards the source. AAPM TG 43 [1] recommended anisotropy values for this source are limited down to 1 cm from the source and do not reproduce the above mentioned anisotropy increase. At larger angles the latter values appear more scattered making it difficult to extract any useful conclusion. Therefore, Chiu-Tsao two-dimensional data could be considered a closer representation of the reality than the currently recommended data.

It was found necessary to model the ^{103}Pd seed model 200 in greater detail, i.e. including a 0.3 mm 103Pd layer around the graphite pellets in order to reproduce experimental measurements of angular radiation distribution in air. Lack of a detailed source design information is probably the cause for remaining discrepancies. Although scattering in water tend to smooth out geometrical source features, such effects are not completely removed and are actually observed in the anisotropy function.

Experimental measurements and Monte Carlo calculations of dose rate distributions around ^{125}I seed model 6711 demonstrate that dose rate values at angles over $50^o$are greater than on the transverse axis for all distances. With increasing distance this effect is shifted towards the transversal axis. When modeling the source without photon emission from the source ends such effect is not observed. A better agreement with experimental values is obtained when the source model of photon emission from the whole silver rod surface is used. It is remarkable the quality of agreement between Monte Carlo simulation and experimental data achieved for ^{125}I seed model 6711. In this case simplicity and a better knowledge of the internal geometrical details of the seed allows for precise computation of the two-dimensional dose distribution around the source in air as well as in water medium, confirming reliability of Monte Carlo simulations.

Use of algorithms for fast dose estimation in clinical practice based on previously measured angular profiles in air should be carefully examined and their validity tested. Sources are "seen" with different grades of detail at different distances. The angular distribution at 100 cm contains less information about the geometrical design of the source than at shorter distances. When using the angular distribution at 100 cm from the source as starting angular distribution from an emitting source the information

is incomplete and an underestimation of the anisotropy near the source is observed. Anisotropy functions in water based on angular distributions measured in air at 100 cm from the source for ^{103}Pd seed model 200 and ^{125}I seed model 6711 fail to reproduce geometrical effects observed in our Monte Carlo data and previous published experimental results.

Insufficient knowledge about source structure is responsible for discrepancies observed in Monte Carlo generated data by different authors. A limited amount of experimental data can be used to validate or optimize the assumed models because of the large experimental errors. Therefore more accurate measurements will be welcome. Accuracy in Monte Carlo calculation of dose rate distributions is limited only by the extent to which the Monte Carlo program can model the physical structures, the physics of the radiation transport through these materials, and the statistical uncertainty of the random process simulated. In order to have a realistic information about the geometric structure, imaging techniques, such as pinhole autoradiography and contact transmission micro-radiography should be used. Statistical fluctuations can be computationally drastically reduced, making a Monte Carlo method an efficient alternative to measured data, once complete and accurate geometrical information is available.

Acknowledgments

We are deeply indebted to Prof. Dr. J. F. Williamson, Prof. Dr. A. Piermattei, Dr. A. S. Meigooni, Dr. A. Bielajew and Dr. R. Wang for useful comments and discussion of relevant problems. Special thanks to Dr. D.W.O. Rogers and Dr. M. C. Schell for the considerable support in accessing key information for the successful conclusion of this work. We also express our gratitude to Dr. Y. Namito who kindly provided us with the LSCAT extension to the EGS4 system and to the whole Organizing Committee for providing financial support, allowing one of us (EM) to present this work.

References

[1] R. Nath, L. L. Anderson, G. Luxton, K. A. Weaver, J. F. Williamson, A. S. Meigooni, "Dosimetry of interstitial brachytherapy sources", Recommendations of the AAPM Radiation Therapy Committee, Task Group 43, *Med. Phys.* **22**(1995)209-234.

[2] C. C. Ling, M. C. Schell and E. D. Yorke, "Two-dimensional dose distribution of ^{125}I seeds", *Med. Phys.* **12**(1985)652-655.

[3] M. C. Schell, C. C. Ling, Z. C. Gromadzki and K. R. Working, "Dose distributions of model 6702 I-125 seeds in water", *Int. J. Radiation Oncology. Biol. Phys.* **13**(1987)795-799.

[4] A. Piermattei, G. Arcovito and B. F. Andreasi, "Experimental dosimetry of I-125 new seeds (mod.6711) for brachytherapy treatments", *Phys. Med.* **1**(1988)59-70.

[5] K. A. Weaver, V. Smith, D. Huang, C. Barnett, M. C. Schell and C. Ling, "Dose parameters of I-125 and Ir-192 seed sources", *Med. Phys.* **16**(1989)636-643.

[6] K. A. Weaver, "Anisotropy functions for ^{125}I and ^{103}Pd sources", *Med. Phys.* **25**(12)(1998) 2271-2278.

[7] R. Nath, A. S. Meigooni and J. A. Meli, "Dosimetry on transverse axes of I-125 and Ir-192 interstitial brachytherapy sources", *Med. Phys.* **17**(1990)1032-1040.

[8] S. T. Chiu-Tsao, L. L. Anderson, K. O'Brien and R. Sanna, "Dose rate determination for I-125 seeds", *Med. Phys.* **17**(1990)817-825.

[9] G. Luxton, M. A. Astrahan, D. O. Findley and Z. Petrovich, "Measurement of dose-rate from exposure calibrated I-125 seeds", *Int. J. Radiat. Oncol. Phys.* **18**(1990)1199-1207.

[10] Interstitial Collaborative Working Group (ICWG), "Interstitial Brachytherapy: Physical, Biological, and Clinical Considerations", ed. L. L. Anderson, R. Nath and K. A. Weaver (Raven, New York), p.21-32, 1990.

[11] A. S. Meigooni, S. Sabnis and R. Nath, "Dosimetry of palladium-103 brachytherapy sources for permanent implants", *Endocurietherapy Hypertherm. Oncol.* **6**(1990)107-117.

[12] S. T. Chiu-Tsao and L. L. Anderson, "Thermoluminiscent dosimetry for Pd-103 (mod.200) in solid water phantom", *Med. Phys.* **18** (1991)449-452.

[13] R. G. Dale, "Some theoretical derivations relating to the tissue dosimetry of brachytherapy nuclides, with particular reference to ^{125}I", *Med. Phys.* **10**(1983)176-183.

[14] J. F. Williamson, F. C. Deibel and R. L. Morin, *Phys. Med. Biol.* **29**(1984)1063.

[15] R. G. Dale, "Revisions to radial dose functions data for ^{125}I and ^{137}Cs", *letter to Med. Phys.* **13**(1986)963-964.

[16] G. Herbolt, G. Hartmann, H. Treuer and W. J. Lorenz, "Monte Carlo calculation of energy buildup factors in the range from 15 to 100 keV with special references to the dosimetry of ^{125}I seeds", *Phys. Med. Biol.* **33**(1988)1037-1053.

[17] G. S. Burns and D. E. Raeside, "Monte Carlo simulation of the dose distribution around ^{125}I seeds", *Med. Phys.* **14**(1987)420-424.

[18] G. S. Burns and D. E. Raeside, "Two-dimensional dose distribution around a commercial ^{125}I seed", *Med. Phys.* **15**(1988)56-60.

[19] J. F. Williamson, "Monte Carlo evaluation of specific dose constant in water for I-125 seeds", *Med. Phys.* **15**(1988)686-694.

[20] J. F. Williamson, "Comparison of measured and calculated dose rates in water near I-125 and Ir-192 seeds", *Med. Phys.* **18**(1991)776-786.

[21] E. C. Scarbrough, G. E. Sanborn, J. A. Anderson, P. D. Nguyen, J. Y. Niederkorn and P. P. Antich, "Dose distribution around a 3.0-mm type 6702 I-125 seed", *Med. Phys.* **17**(1990)460-463.

[22] G. Luxton, "Comparison of radiation dosimetry in water and in solid phantom materials for I-125 and Pd-103 brachytherapy sources: EGS4 Monte Carlo study", *Med. Phys.* **21**(1994)631-641.

[23] R. Wang and R. Slovoda, "EGS4 dosimetry calculations for cylindrically symmetric brachytherapy sources", *Med. Phys.* **23**(1996)1459-1465.

[24] E. Mainegra, R. Capote, E. López, "Dose rate constants for ^{125}I, ^{103}Pd, ^{192}Ir and ^{169}Yb brachytherapy sources: An EGS4 Monte Carlo study", *Phys. Med. Biol.* **43**(1998)1557-1566.

[25] E. Mainegra, R. Capote, E. López, "Radial Dose Functions for ^{103}Pd, ^{125}I, ^{169}Yb and ^{192}Ir Brachytherapy Sources: An EGS4 Monte Carlo study", *Phys. Med. Biol.* **45**(2000)703-717.

[26] J. F. Williamson and R. Nath, "Clinical implementation of AAPM task group 32 recommendations on brachytherapy source strength specification", *Med. Phys.* **18**(1991)439-448.

[27] Brookhaven National Laboratory, NUDAT database, last update 01/31/96, National Nuclear Data Center, Upton, N.Y., USA, 1996.

[28] A. S. Meigooni, J. A. Meli, and R. Nath, "A comparison of solid phantoms with water for dosimetry of ^{125}I brachytherapy sources", *Med. Phys.* **15**(1988)695-701.

[29] W. R. Nelson, H. Hirayama and D. W. O. Rogers, "The EGS4 code system, Version 4", Stanford Linear Accelerator Center Report *SLAC-265*, 1985.

[30] W. R. Nelson and D. W. W. Rogers, "Monte Carlo transport of electrons and photons", ed. T. M. Jenkins, W. R. Nelson and A. Rindi (Plenum, New York) pp.287-306, 1988.

[31] RSIC Data Package *DLC-136/PHOTX* by National Institute of Standards and Technology, 1993.

[32] Y. Sakamoto, Proc. Third EGS4 User's Meeting in Japan, KEK Proceedings 93-15, 1993.

[33] J. H. Scoffield, "Theoretical Photoionization cross sections from 1 to 1500 KeV", Lawrence Livermore Laboratory, Livermore CA., *UCRL-51326*, 1973.

[34] Y. Namito, S. Ban and H. Hirayama, *Nucl. Instr. Meth.* **A349**(1994)489-494; *KEK Internal Report 95-10*, 1995.

[35] L. R. M. Morin, *J. Phys. Chem. Ref. Data.* **11**(1982)1091-1098.

[36] C. J. Leliveld, J. G. Maas, V. R. Bom and C. W. E. Van Eijk, presented at the IEEE Medical Imaging Conference, October 26-28, San Francisco, 1995.

[37] A. F. Bielajew and D. W. O. Rogers, "DOSRZ user code", EGS4 distribution package, 1989.

[38] T. P. Loftus, *J. Res. Natl. Bur. Stand.* **89**(1984)295-303.

[39] D. L. D. Mason, J. J. Battista, R. B. Barnett and A. T. Porter, *Med. Phys.* **19**(1992)695-703.

[40] S. M. Seltzer, P. J. Lamperti, R. Loevinger, C. G. Soares, and J. T. Weaver, "New NIST air-kerma strength standards for I-125 and Pd-103 brachytherapy seeds", Poster presentation, AAPM Annual Meeting, August 1998, San Antonio, TX (Abstract: *Med Phys.* **25**(1998)A170.).

[41] J. F. Williamson, B. M. Courtsey, L. A. DeWerd, W. F. Hanson, R. Nath, M. J. Rivard and G. Ibbot, Draft of AAPM Report 69, to be published in Medical Physics 2000.

[42] R. Nath, N. Yue, K. Shahnazi and P. J. Bongiorni, "Measurement of dose-rate constant for ^{103}Pd seeds with air-kerma strength calibration based upon a primary national standard", *Medical Physics* submitted 9/99 (1999).

[43] J. F. Williamson, "Monte Carlo modeling of the transverse-axis dose distribution of the model 200 ^{103}Pd interstitial brachytherapy source", *Medical Physics* submitted 12/99 (1999).

[44] R. Capote and E. Mainegra, "Anisotropy functions for low energy interstitial brachytherapy sources: An EGS4 Monte Carlo study", *Phys. Med. Biol.* submitted 4/2000 (2000).

[45] R. Nath, A. S. Meigooni, P. Muench and A. Melillo, *Med. Phys.* **20**(1993)1465-1473.

[46] K. A. Weaver, C. H. Siantar, W. Chandler and R. M. White, *Med. Phys.* **23 (12)**(1996)2079-2084.

[47] J. F. Williamson and F. J. Quintero, *Med. Phys.* **15** (1983)891-897.

[48] C. C. Ling, E. D. Yorke, I. J. Spiro, D. Kubiatowics and D. Bennett, *Int. J. Radiation Oncology. Biol. Phys.* **9**(1983)1747-1752.

Table 1 Dose rate constants for ^{125}I seeds.

Author (Cross section library)	Air-kerma strength	Phantom Material	Λ [cGy h^{-1} U^{-1}] model 6702	Λ [cGy h^{-1} U^{-1}] model 6711
Williamson 1988, Ref.45 (DLC-7F)	S_k in air	Atomic water	0.962	0.909
This study 1998, Ref.24 (DLC-15)	**S_k in air**	**Atomic water**	**0.96 ± 0.04**	**0.89 ± 0.01**
	S_k in vacuum	**Atomic water**	**0.83 ± 0.02**	**0.73 ± 0.01**
Mason 1992, Ref.39, (DLC-99)	S_k in vacuum	Atomic water	0.82 ± 0.04	---
	S_k in air	Atomic water	0.93 ± 0.04	---
Wang *et al* 1996, Ref.23 (DLC-99)	S_k in air	atomic water	---	0.895 ± 0.004
Williamson 1991, Ref.20 (DLC-99)	S_k in air	liquid water	0.932	0.877
		solid water	0.899	0.841
This study, Ref.24 (DLC-136)	**S_k in air**	**liquid water**	**0.933 ± 0.002**	**0.888 ± 0.002**
		solid water	**0.908 ± 0.004**	**0.858 ± 0.004**
Piermattei *et al* 1988, Ref.4	Measurements	MS11(water)	---	0.890
Luxton *et al* 1990, Ref.9	Measurements	PMMA	---	0.984
Luxton 1994 (correction), Ref.24	---	liquid water	---	0.879
NCI contract group				
Nath *et al* 1990, Ref.7	Measurements	solid water	0.903	0.855
Weaver *et al* 1989, Ref.5	Measurements	solid water	0.923	0.832
Chiu-Tsao *et al* 1990, Ref.8	Measurements	solid water	0.932	0.853
ICWG average 1990, Ref.10	---	solid water	0.919	0.847

Table 2. Anisotropy Function for a ^{125}I seed model 6711.

R[cm]/θ[deg]	0	10	20	30	40	50	60	70	80
0.50	0.2307	0.3770	0.6246	0.8239	0.9435	1.0009	1.0338	1.0460	0.9897
1.0	0.3130	0.4820	0.7006	0.8396	0.9279	0.9893	1.0247	1.0394	1.0417
1.5	0.3762	0.5359	0.7345	0.8495	0.9284	0.9832	1.0196	1.0334	1.0383
2.0	0.4230	0.5741	0.7532	0.8573	0.9285	0.9808	1.0143	1.0307	1.0357
2.5	0.4403	0.5967	0.7546	0.8412	0.9074	0.9549	0.9925	1.0175	1.0302
3.0	0.4753	0.6204	0.7743	0.8614	0.9170	0.9652	0.9996	1.0173	1.0281
3.5	0.4938	0.6389	0.7836	0.8668	0.9244	0.9663	1.0008	1.0166	1.0264
4.0	0.5137	0.6531	0.7906	0.8693	0.9245	0.9681	0.9993	1.0168	1.0242
4.5	0.5417	0.6649	0.7971	0.8736	0.9284	0.9690	0.9987	1.0166	1.0235
5.0	0.5652	0.6753	0.8020	0.8740	0.9289	0.9688	0.9976	1.0140	1.0232
5.5	0.5672	0.6859	0.8057	0.8776	0.9290	0.9686	0.9942	1.0133	1.0205
6.0	0.5828	0.6945	0.8107	0.8807	0.9332	0.9698	0.9978	1.0145	1.0208
6.5	0.5760	0.6996	0.8126	0.8830	0.9322	0.9688	0.9944	1.0104	1.0193
7.0	0.5776	0.7066	0.8150	0.8832	0.9324	0.9690	0.9951	1.0103	1.0168
7.5	0.6439	0.7147	0.8154	0.8846	0.9325	0.9677	0.9929	1.0079	1.0160
8.0	0.6439	0.7150	0.8183	0.8837	0.9317	0.9672	0.9928	1.0052	1.0134
8.5	0.6594	0.7238	0.8230	0.8876	0.9337	0.9703	0.9934	1.0089	1.0165
9.0	0.6041	0.7312	0.8250	0.8895	0.9374	0.9714	0.9955	1.0102	1.0171

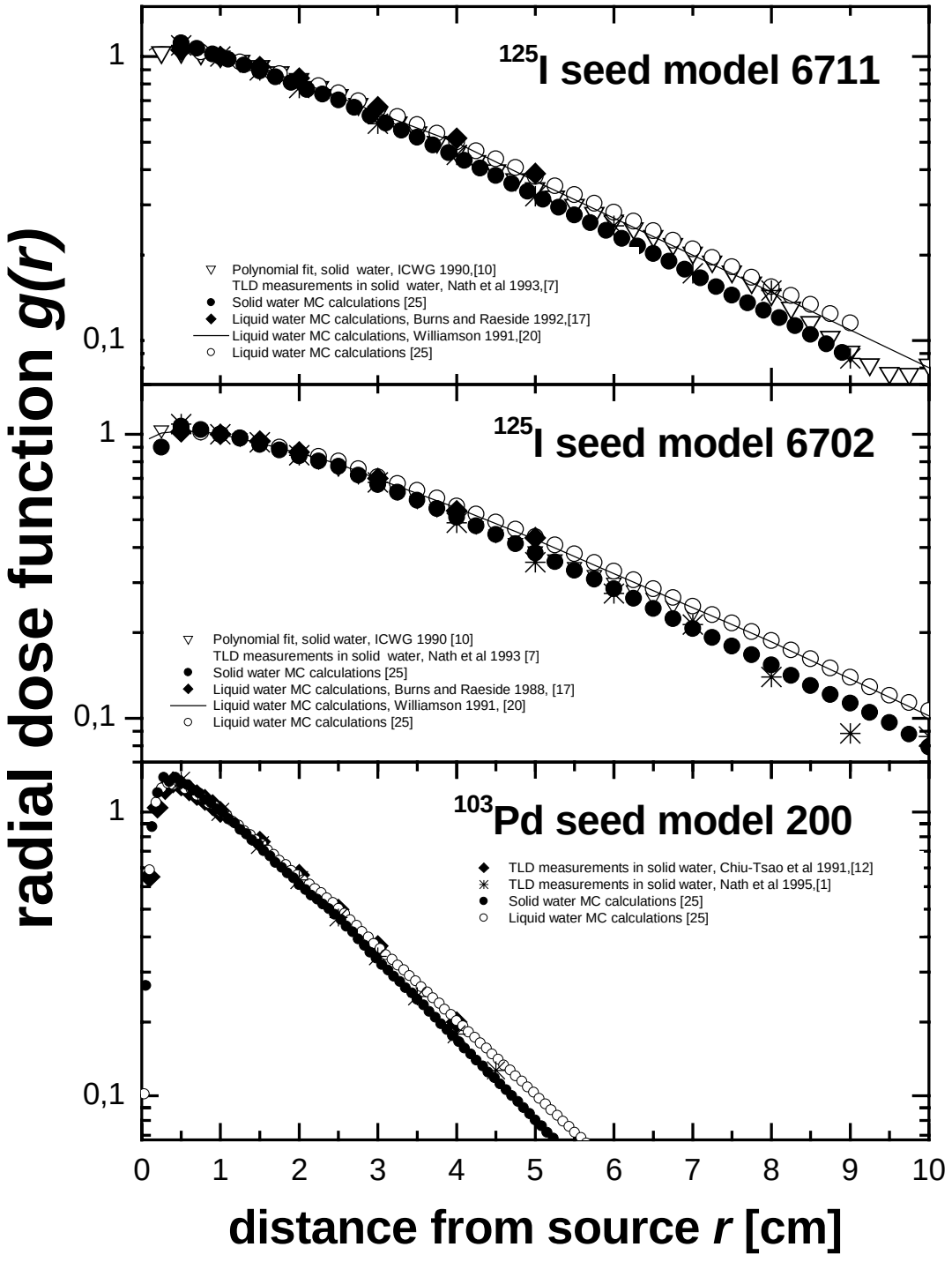

Figure 1: Calculated radial dose functions *g(r)* for low-energy brachytherapy seeds in liquid and solid water compared with experimental measurements in solid water phantoms.

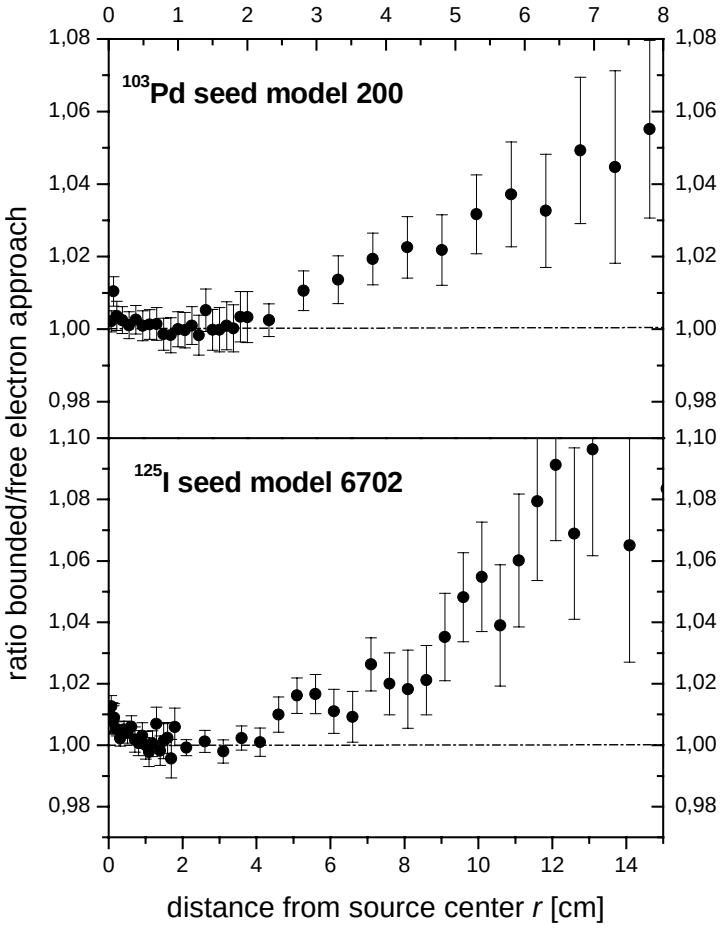

Figure 2: Influence of Compton binding corrections on radial dose function for low energy brachytherapy seeds. The ratio of radial dose functions with and without the corrections is plotted as a function of distance on transverse axis.

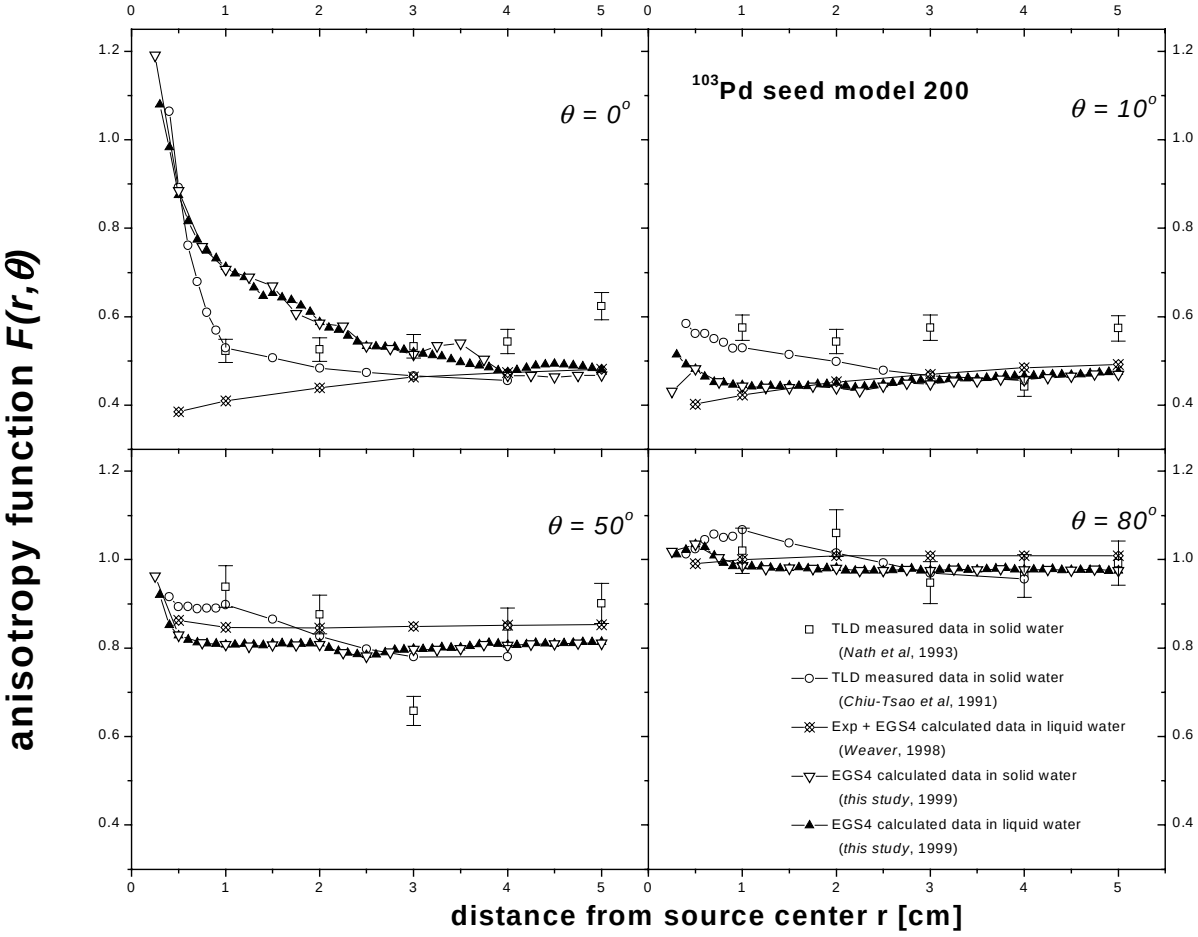

Figure 3: Anisotropy function for a ^{103}Pd seed model 200 as function of distance.

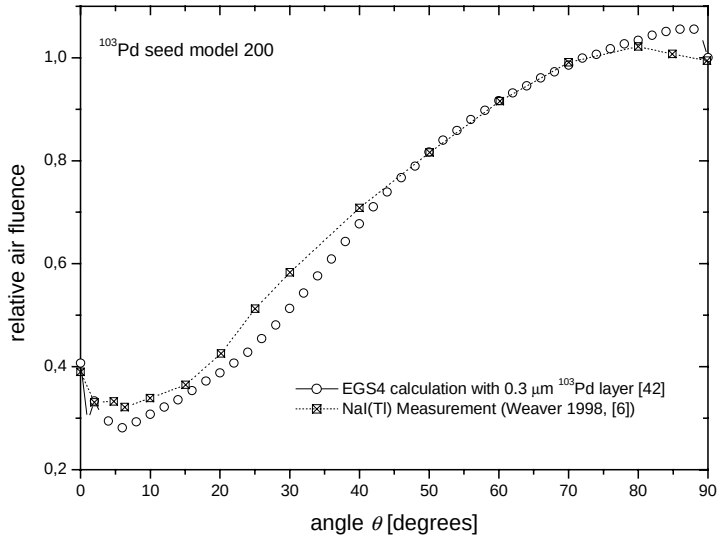

Figure 4: Comparison of relative in air fluence for ^{103}Pd seed model 200 obtained from our EGS4 calculations with measurements of Weaver [6].

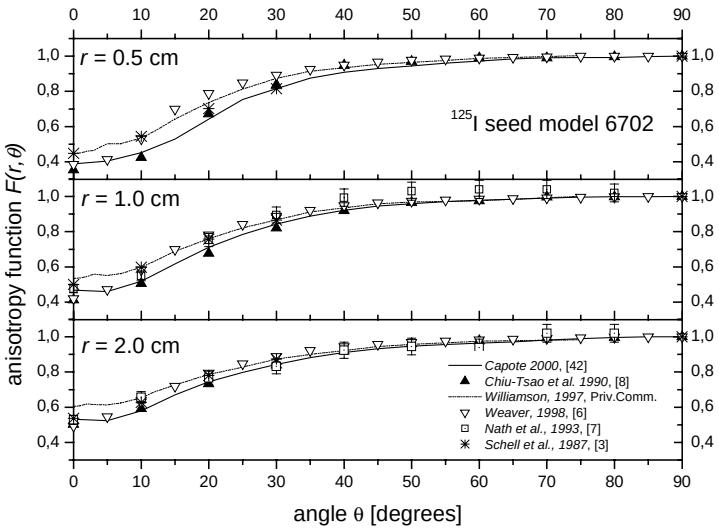

Figure 5: Anisotropy Function for a ^{125}I seed model 6702 as function of angle. Diode measurements in liquid water are represented with a star, TLD measurements in solid water with an open square, EGS4 calculations based on experimental determined angular emission distributions with an open triangle, calculations using MORSE code with a solid triangle, MCPT calculations with dotted line and full EGS4 calculations with a solid line.

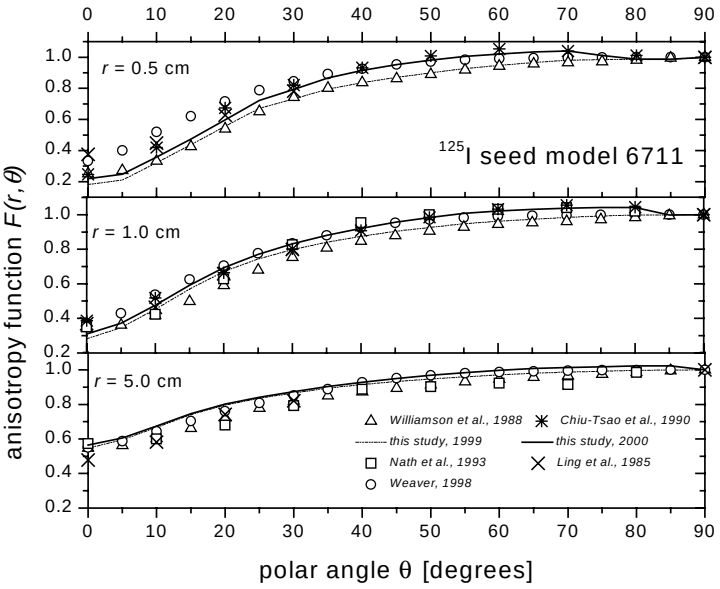

Figure 6: Anisotropy Function for a ^{125}I seed model 6711 as function of angle. Diode measurements in liquid water are represented with a cross, TLD measurements in solid water with an open square, EGS4 calculations based on experimental determined angular emission distributions with an open circle, MCPT calculations with an open triangle and full EGS4 calculations for a partially and a whole emitting source with a dashed and a solid line respectively.

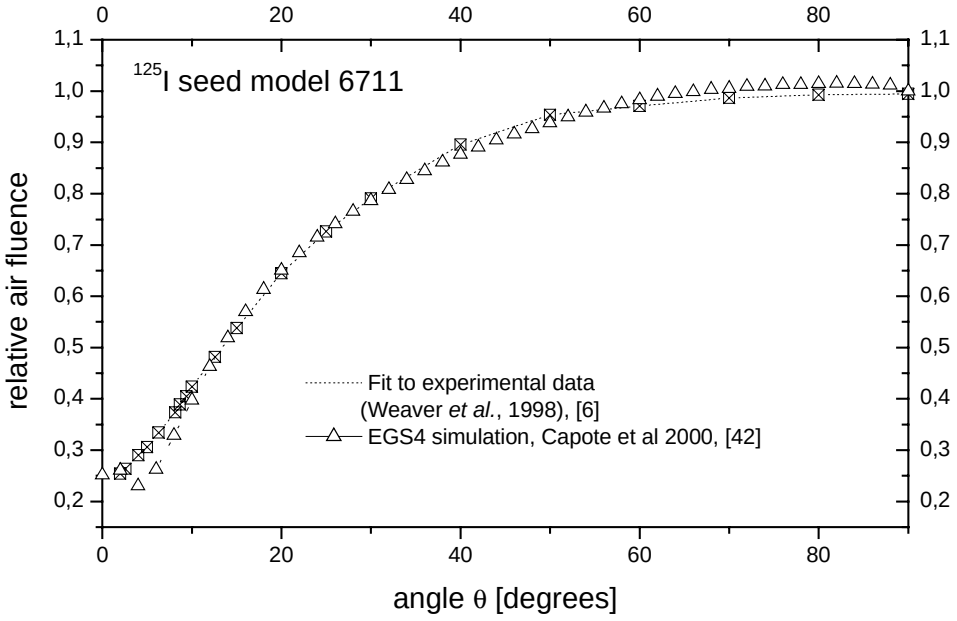

Figure 7: Relative air fluence at 100 cm for a ^{125}I seed model 6711.